Available online at www.sciencedirect.com
SCIENCE DIRECT®
C. R. Mecanique 332 (2004) 987–992
COMPTES RENDUS MECANIQUE
http://france.elsevier.com/direct/CRAS2B/

On the slow gravity-driven migration of arbitrary clusters of small solid particles

Antoine Sellier

LadHyX, École polytechnique, 91128 Palaiseau cedex, France

Received 29 June 2004; accepted after revision 2 September 2004

Available online 2 November 2004

Presented by Évariste Sanchez-Palencia

Abstract

A new approach is advocated to compute at a low cpu time cost the rigid-body motions of settling solid particles when inertial effects are negligible. In addition to the relevant boundary-integral equations, the numerical implementation and a few convincing benchmark tests we address two configurations of equivalent spheres and spheroids, i.e. that exhibit when isolated the same settling velocity. ***To cite this article: A. Sellier, C. R. Mecanique 332 (2004).***

Résumé

Sur la sédimentation d'une assemblée quelconque de particules solides. On propose une approche originale pour déterminer le mouvement d'une assemblée de particules solides et de formes arbitraires soumise à l'action de la pesanteur dans l'approximation de Stokes. Outre les intégrales de frontière et la méthode numérique associées on présente quelques comparaisons et examine le cas de deux configurations de sphères et ellipsoides de révolution équivalents, c'est-à-dire dotés lorsqu'ils sont seuls de la même vitesse de sédimentation. ***Pour citer cet article : A. Sellier, C. R. Mecanique 332 (2004).***

Keywords: Fluid mechanics; Sedimentation; Particle–particle interactions; Boundary-integral

Mots-clés : Mécanique des fluides ; Sédimentation ; Interactions ; Équations de frontière

1. Introduction

Evaluating the rigid-body motion(s) of $N \geqslant 1$ arbitrarily-shaped solid particles subject to the gravity and adopting a general (not necessary periodic) configuration remains a tremendous task even within the usual Stokes flow

E-mail address: sellier@ladhyx.polytechnique.fr (A. Sellier).

1631-0721/$ – see front matter
doi:10.1016/j.crme.2004.09.002

approximation. Consequently, the available works only deal with spheres [1–4] or axisymmetric chains of spheroids aligned with the gravity [5,6]. This study thus introduces a new method valid whatever the shapes of the particles. The advocated approach appeals to $6N$ boundary-integral equations and makes it possible to calculate the rigid-body of each particle without determining the unbounded fluid flow about the cluster.

2. General theory

We consider, as depicted in Fig. 1, a collection of $N \geqslant 1$ arbitrarily-shaped solid, small and not necessarily homogeneous particles $\mathcal{P}_n$ with surface S_n, center of mass O_n and mass M_n. Using Cartesian coordinates (O, x_1, x_2, x_3) and the usual tensor summation convention with $\mathbf{OM} = x_i \mathbf{e}_i$, we assume that the particles are subject to the uniform gravity field $\mathbf{g} = -g\mathbf{e}_3$ (with $g > 0$) and immersed in a quiescent and unbounded Newtonian fluid of uniform viscosity μ and density ρ.

The solid $\mathcal{P}_n$ with small length scale a_n experiences a quasi-static rigid-body motion of unknown angular velocity $\mathbf{\Omega}^{(n)}$ and translational velocity $\mathbf{U}^{(n)}$ (the velocity of O_n). Neglecting inertial effects, i.e. assuming that $\mathrm{Re} = \rho U a/\mu \ll 1$ with $a = \mathrm{Max}(a_n)$ and $U = \mathrm{Max}(|\mathbf{U}^{(n)}|, a_n|\mathbf{\Omega}^{(n)}|)$, the quasisteady fluid velocity field $\mathbf{u}$ and pressure field $p + \rho g x_3$ obey

$$\mu \nabla^2 \mathbf{u} = \nabla p \quad \text{and} \quad \nabla.\mathbf{u} = 0 \quad \text{in } \Omega \tag{1}$$

$$(\mathbf{u}, p) \to (\mathbf{0}, 0) \quad \text{as } r = (x_i x_i)^{1/2} \to \infty, \qquad \mathbf{u} = \mathbf{U}^{(n)} + \mathbf{\Omega}^{(n)} \wedge \mathbf{O_nM} \quad \text{on } S_n \tag{2}$$

with Ω the fluid domain. The generalized velocity $\mathbf{X} := (\mathbf{U}^{(1)}, \ldots, \mathbf{U}^N; \mathbf{\Omega}^{(1)}, \ldots, \mathbf{\Omega}^{(N)})$ is unknown and one thus needs to supplement (1)–(2) with additional relations. Denoting by $\mathbf{n}$ the unit outward normal on S_n, the flow $(\mathbf{u}, p)$ with stress tensor σ, the static pressure $\rho g x_3$ and the gravity $\mathbf{g}$ apply on $\mathcal{P}_n$ with volume $\mathcal{V}_n$ and center of volume O'_n a net force $\mathbf{R}^{(n)}$ and a net torque $\mathbf{C}^{(n)}$ (about the center of mass O_n) such that

$$\mathbf{R}^{(n)} = \int_{S_n} \sigma.\mathbf{n}\,\mathrm{d}S_n + (M_n - \rho\mathcal{V}_n)\mathbf{g}, \qquad \mathbf{C}^{(n)} = \int_{S_n} \mathbf{O_nM} \wedge \sigma.\mathbf{n}\,\mathrm{d}S_n - \rho\mathcal{V}_n \mathbf{O_nO'_n} \wedge \mathbf{g} \tag{3}$$

Neglecting particle inertia, the required conditions read $\mathbf{R}^{(n)} = \mathbf{C}^{(n)} = \mathbf{0}$, i.e.

$$\mathbf{F}^{(n)} := \int_{S_n} \sigma.\mathbf{n}\,\mathrm{d}S_n = (\rho\mathcal{V}_n - M_n)\mathbf{g}, \qquad \mathbf{\Gamma}^{(n)} := \int_{S_n} \mathbf{O_nM} \wedge \sigma.\mathbf{n}\,\mathrm{d}S_n = \rho\mathcal{V}_n \mathbf{O_nO'_n} \wedge \mathbf{g} \tag{4}$$

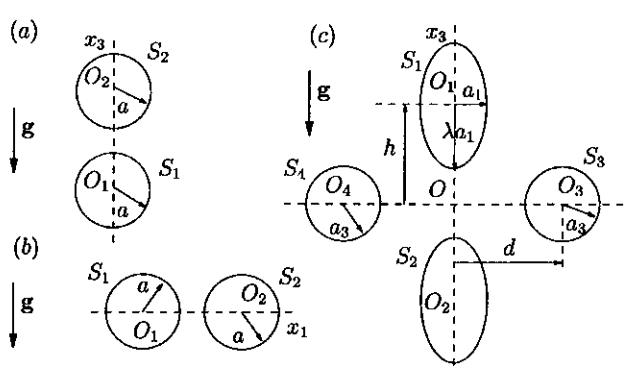

Fig. 1. A 2-sphere cluster in (a) axisymmetric or (b) asymmetric cases and (c) a cluster of 4 equivalent spheres and spheroids.

Fig. 1. Deux sphères disposées de façon (a) axisymétrique ou (b) asymétrique et (c) un ensemble de 4 sphères et ellipsoides de révolution équivalents.

When determining $\mathbf{X}$ fulfilling (1), (2) and (4) one may think about using a Finite Element Method to calculate the above net forces $\mathbf{F}^{(n)}$ and torques $\mathbf{\Gamma}^{(n)}$ induced by $(\mathbf{u}, p)$ solution to (1), (2) for a given guess value $\mathbf{X}_g$ and then iteratively modify $\mathbf{X}_g$ until (4) is satisfied. Unfortunately, for fully three-dimensional N-particle clusters this strategy is tremendously cpu time consuming and yields a poor accuracy for the velocity $\mathbf{X}$ because one has to numerically evaluate the traction $\boldsymbol{\sigma}.\mathbf{n}$ on each boundary S_n for the computed flow $(\mathbf{u}, p)$. The approach advocated in this work is free from such drawbacks and appeals to $6N$ steady Stokes flows $(\mathbf{u}_L^{(n),i}, p_L^{(n),i})$ with $L \in \{T, R\}$, $i \in \{1, 3\}$ and $n \in \{1, \ldots, N\}$. These flows, free from body force and quiescent far from the cluster, obey (1) and the boundary conditions

$$\mathbf{u}_T^{(n),i} = \delta_{nm}\mathbf{e}_i, \quad \mathbf{u}_R^{(n),i} = \delta_{nm}[\mathbf{e}_i \wedge \mathbf{O_n M}] \quad \text{on } S_m \tag{5}$$

with δ_{nm} the Kronecker symbol. The flow $(\mathbf{u}_L^{(n),i}, p_L^{(n),i})$ has stress tensor $\boldsymbol{\sigma}_L^{(n),i}$ and thus applies the surface traction $\mathbf{f}_L^{(n),i} = \boldsymbol{\sigma}_L^{(n),i}.\mathbf{n}$ on the entire cluster's boundary $S = \bigcup_{n=1}^N S_n$. Noting that, since $(\mathbf{u}, p)$ obeys (1), the usual reciprocal theorem [7] yields

$$\int_S \mathbf{u}_L^{(n),i}.\boldsymbol{\sigma}.\mathbf{n}\,\mathrm{d}S = \int_S \mathbf{u}.\boldsymbol{\sigma}_L^{(n),i}.\mathbf{n}\,\mathrm{d}S = \int_S \mathbf{u}.\mathbf{f}_L^{(n),i}\,\mathrm{d}S \tag{6}$$

it is then straightforward, by exploiting the boundary conditions (2) and (5), to cast the conditions (4) under the following $6N$-equation linear system

$$A_{(m),T}^{(n),i,j} U_j^{(m)} + B_{(m),T}^{(n),i,j} \Omega_j^{(m)} = (\rho \mathcal{V}_n - M_n) g \delta_{i3}/\mu \tag{7}$$

$$A_{(m),R}^{(n),i,j} U_j^{(m)} + B_{(m),R}^{(n),i,j} \Omega_j^{(m)} = \rho g \mathcal{V}_n \big(\mathbf{O_n O'_n} \wedge \mathbf{e}_3\big).\mathbf{e}_i/\mu \tag{8}$$

if one sets $U_j^{(m)} = \mathbf{U}^{(m)}.\mathbf{e}_j$, $\Omega_j^{(m)} = \boldsymbol{\Omega}^{(m)}.\mathbf{e}_j$ and makes use of the definitions

$$-\mu A_{(m),L}^{(n),i,j} = \int_{S_m} \mathbf{e}_j.\mathbf{f}_L^{(n),i}\,\mathrm{d}S_m, \qquad -\mu B_{(m),L}^{(n),i,j} = \int_{S_m} (\mathbf{e}_j \wedge \mathbf{O_m M}).\mathbf{f}_L^{(n),i}\,\mathrm{d}S_m \tag{9}$$

The key system (7), (8) admits a $6N \times 6N$ square, real-valued, symmetric and positive-definite matrix [8] and therefore a unique solution $\mathbf{X}$ for any N-particle cluster and settings $\mathcal{P}_n$, ρ_n, M_n, $\mathcal{V}_n$, O_n, O'_n. It also shows that is sufficient to compute the very few surface tractions $\mathbf{f}_L^{(n),i}$ on the entire cluster's boundary S to obtain the required rigid-body motions of the particles. As nicely established in [9], the velocity field $\mathbf{u}_L^{(n),i}$ admits both in the unbounded fluid domain Ω and on the surface S the integral representation

$$\big[\mathbf{u}_L^{(n),i}.\mathbf{e}_k\big](M) = -\int_S \left\{\frac{\delta_{jk}}{PM} + \frac{(\mathbf{PM}.\mathbf{e}_j)(\mathbf{PM}.\mathbf{e}_k)}{PM^3}\right\}\left[\frac{\mathbf{f}_L^{(n),i}.\mathbf{e}_j}{8\pi\mu}\right](P)\,\mathrm{d}S \quad \text{for } k = 1, 2, 3 \tag{10}$$

The proposed strategy then consists of the following steps:

(i) First, obtain each traction $\mathbf{f}_L^{(n),i}$ by exploiting the representation (10) on S. One thus ends up with a Fredholm boundary-integral equation of the first kind that admits a solution defined up to an arbitrary constant multiple of $\mathbf{n}$ on each subdomain S_n [9].

(ii) Solve the governing system (7)–(8) by computing the coefficients $A_{(m),L}^{(n),i,j}$ and $B_{(m),L}^{(n),i,j}$ (which are readily uniquely determined for $\mathbf{f}_L^{(n),i}$ defined up to a multiple of $\mathbf{n}$ on S_m).

(iii) If needed, evaluate the velocity $\mathbf{u}$ in the unbounded domain Ω by using (10) where $\mathbf{u}_L^{(n),i}$ and $\mathbf{f}_L^{(n),i}$ are replaced with $\mathbf{u}$ and $\mathbf{f} = \sum_{n=1}^N \sum_{i=1}^3 \{U_i^{(n)} \mathbf{f}_T^{(n),i} + \Omega_i^{(n)} \mathbf{f}_R^{(n),i}\}$, respectively.

Clearly, the advocated approach applies to N-particle clusters made of arbitrarily-shaped and not necessarily homogeneous particles. Moreover, the derived boundary formulation permits us in practice to accurately compute the rigid-body motions of the particles without determining the fluid flow (by only using the previous steps (i)–(ii)).

3. Numerical implementation and benchmarks

The $6N$ boundary-integral equations encountered in step (i) are discretized by using on S_n a $N_d^{(n)}$-node mesh of 6-node isoparametric, curvilinear triangular and boundary elements [10,9]. This results in a N_d-node mesh on the cluster's surface S and the obtained linear systems with dense and non-symmetric $3N_d \times 3N_d$ matrix are solved by Gaussian elimination. Henceforth, we confine the analysis to the case of homogeneous ($O_n = O'_n$) spheres and spheroids. Appealing to [8], a single spheroid $\mathcal{P}_1$ of inequation $x_1^2 + x_2^2 + x_3^2/\lambda^2 \leqslant a_1^2$ is found to settle without rotating at the velocity $\mathbf{U}^{(1)} = g a_1^2(\rho - \rho_1)v\mathbf{e}_3/\mu$ with $v = 2/9$ for a sphere and for $\lambda \neq 1$, under the notation $p = \lambda|\lambda^2 - 1|^{-1/2}$,

$$v = \frac{p}{12}\left\{(p^2+1)\log\left[\frac{p+1}{p-1}\right] - 2p\right\} \quad \text{if } \lambda > 1, \qquad v = \frac{p}{6}\left\{p + (1-p^2)\arctan\left(\frac{1}{p}\right)\right\} \quad \text{if } \lambda < 1 \tag{11}$$

Our numerical implementation is benchmarked against the above exact solution for a sphere and oblate ($\lambda = 1/2$) or prolate ($\lambda = 2$) spheroids. As shown in Table 1, the computed velocity v nicely converges towards its analytical value as the number $N_d^{(1)}$ of collocation points on S_1 increases with an excellent relative precision of order of 0.1% for $N_d^{(1)} = 242$. Even for $N_d^{(1)} = 74$, each computed angular velocity component is of order of 10^{-5}.

The case of two identical spheres ($\lambda_1 = \lambda_2 = 1, a_1 = a_2 = a, \rho_1 = \rho_2$) in axisymmetric and asymmetric configurations (see Fig. 1(a), (b)) is also compared with [1] and [2], respectively. Following those works, we list in

Table 1
Computed, normalized velocity v for a sphere and oblate or prolate spheroids using different numbers $N_d^{(1)}$ of collocation points

Tableau 1
Vitesse adimensionnée v obtenue pour une sphère ou des ellipsoids de révolution en utilisant un maillage à $N_d^{(1)}$ nœuds

$N_d^{(1)}$	v ($\lambda = 1/2$)	v ($\lambda = 1$)	v ($\lambda = 2$)
74	0.123016	0.222682	0.370022
242	0.122767	0.222279	0.369245
1058	0.122736	0.222227	0.369164
exact	0.122733	0.222222	0.369158

Table 2
Computed non-zero normalized velocity components $u_3^{(n)}$ and $w_2^{(n)}$ of two identical spheres ($a_1 = a_2 = a$) settling in the (a) axisymmetric and (b) asymmetric configurations sketched in Fig. 1 for two separation parameters $h = O_1O_2/(a_1 + a_2)$

Tableau 2
Vitesses adimensionnées $u_3^{(n)}$ et $w_2^{(n)}$ de deux sphères identiques ($a_1 = a_2 = a$) dans les configurations (a) axisymétrique et (b) asymétrique illustrées à la Fig. 1 pour deux valeurs de la séparation $h = O_1O_2/(a_1 + a_2)$

$N_d^{(1)} = N_d^{(2)}$	h	(a) $u_3^{(1)} = u_3^{(2)}$	(b) $u_3^{(1)} = u_3^{(2)}$	(b) $w_2^{(1)} = -w_2^{(2)}$
74	1.12763	1.51843	1.36702	0.13084
242	1.12763	1.51628	1.36506	0.13154
1058	1.12763	1.51601	1.36481	0.13142
exact [1,2]	1.12763	1.51599	1.36480	0.13141
74	2.35241	1.30458	1.16645	0.03358
242	2.35241	1.30272	1.16435	0.03380
1058	2.35241	1.30248	1.16413	0.03383
exact [1,2]	2.35241	1.30246	1.16410	0.03383

Table 2 the non-zero Cartesian velocity components normalized by the settling velocity of an isolated sphere, i.e. the quantities

$$u_3^{(n)}(h) = \frac{9\mu \mathbf{U}^{(n)}.\mathbf{e}_3}{2g(\rho-\rho_n)a_n^2}, \qquad w_2^{(n)}(h) = \frac{9\mu \boldsymbol{\Omega}^{(n)}.\mathbf{e}_2}{2g(\rho-\rho_n)a_n^3}, \qquad h = \frac{O_1O_2}{a_1+a_2} \tag{12}$$

Again, using 242-node meshes yields a nice 4-digit accuracy even for $h = 1.12763$.

4. Results for configurations of homogeneous equivalent spheres and spheroids

We present preliminary results for two N-particle clusters ($N = 4, 5$) consisting (see Fig. 1(c)) of $N-2$ equal spheres $\mathcal{P}_n$ arranged at the corners of a regular polygon in the horizontal $x_3 = 0$ plane with $3 \leqslant n \leqslant N$, $a_n = a_3$, $OO_n = d$ and two identical spheroids $\mathcal{P}_1$ and $\mathcal{P}_2$ of inequations $x_1^2 + x_2^2 + [x_3 + (-1)^n h]^2 \leqslant \lambda^2 a_1^2$ for $n = 1, 2$ with (λ, d, h) so that the particles do not touch. All the particles admit the same uniform density ρ_s and settling velocity when isolated (equivalent particles), i.e. $a_1/a_3 = (9v/2)^{-1/2}$ with v given by (11) and we resort to a 242-node mesh on each S_n. Symmetries show that the only non-zero normalized Cartesian velocity components are $u^{(1)} = u^{(2)}$ and $u^{(3)} = \cdots = u^{(N)}$ with $u^{(n)} = 9\mathbf{U}^{(n)} \cdot \mathbf{e}_3/[2ga_3^2(\rho - \rho_s)]$ for $n = 1, \ldots, N$.

These quantities are plotted in Fig. 2 versus the ratio $h/a_3 \geqslant 2$ for $d/a_3 = 2$, $\lambda = 0.5, 2$ and $N = 4, 5$. Note that each particle moves faster than if isolated ($u^{(n)} > 1$) and the interactions become strong for $h \sim d = 2a_3$ (with $u^{(n)} \sim 2$). The velocities are bigger for five particles ($N = 5$) than for four particles ($N = 4$) and for a given value of N it is found that $u^{(1)}$ and $u^{(3)}$ weakly and strongly decrease with λ, respectively. Finally, curves for $u^{(1)}$ and $u^{(3)}$ cross for a critical value $h = h_c$ at which the cluster keeps a steady configuration when falling, all particles adopting the same velocity.

The critical setting h_c/d has been found by an iterative (bisection) scheme stopping as soon as $|u^{(1)} - u^{(3)}| \leqslant 5 \times 10^{-4}$ for $1.5 \leqslant d \leqslant 10$ and both the computed ratio h_c/d and the associated cluster's settling velocity $u_c = u^{(1)} = u^{(3)}$ are displayed in Fig. 3. The curves h_c/d previously given in [4] for spheres ($\lambda = 1$) are perfectly recovered and as d increases h_c/d increases and asymptotes to a constant value because particles behave like point forces for large distances d and h. Moreover, h_c/d increases both with λ and N for a given value of d. As revealed by Fig. 3(b), u_c not only increases with d because interactions become strong but also with $1/\lambda$ and N for a

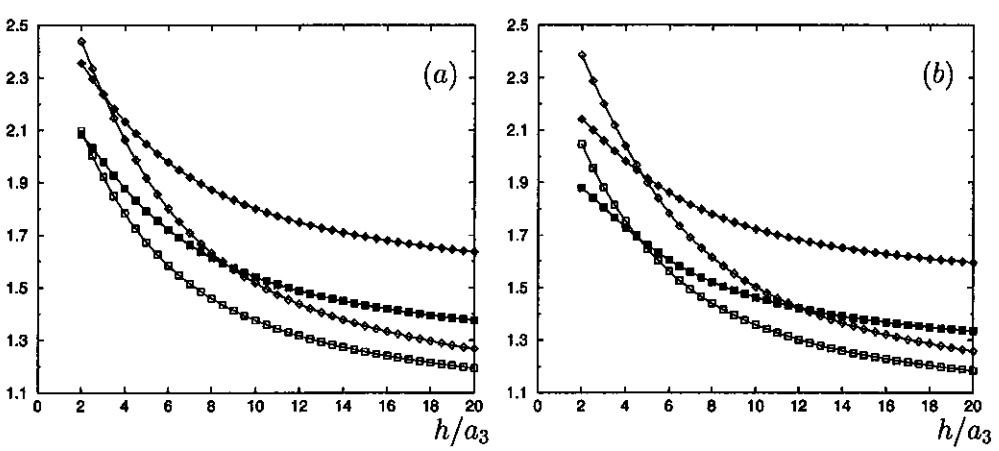

Fig. 2. Normalized velocities $u^{(1)}$ ($N = 4$(□) or $N = 5$(■)) and $u^{(3)}$ ($N = 4$(◊) or $N = 5$(♦)) for $d/a_3 = 2$, (a) $\lambda = 0.5$ and (b) $\lambda = 2$.

Fig. 2. Vitesses adimensionnées $u^{(1)}$ ($N = 4$(□) ou $N = 5$(■)) et $u^{(3)}$ ($N = 4$(◊) ou $N = 5$(♦)) pour $d/a_3 = 2$, (a) $\lambda = 0, 5$ et (b) $\lambda = 2$.

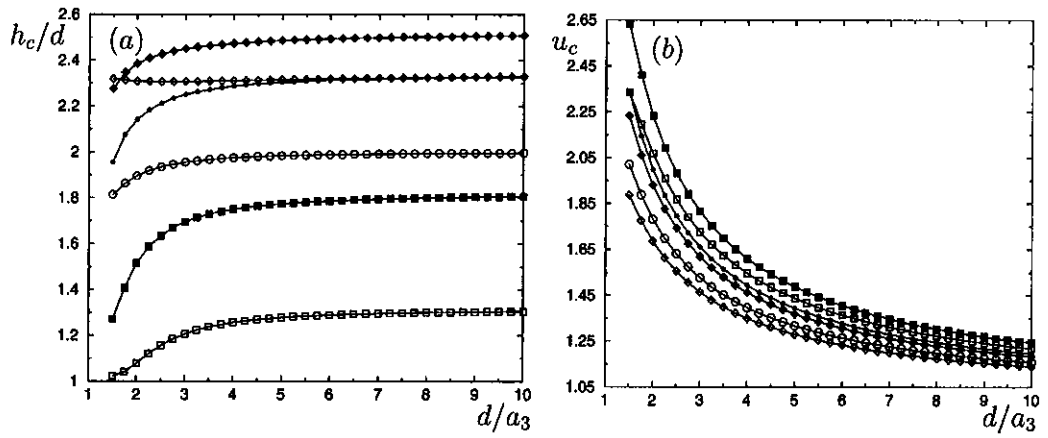

Fig. 3. (a) Critical ratio h_c/d, and (b) settling velocity u_c, of the steady configurations for $\lambda = 0.5$ ($N = 4$(□) or $N = 5$(■)), $\lambda = 1$ ($N = 4$(○) or $N = 5$(●)) and $\lambda = 2$ ($N = 4$(◇) or $N = 5$(◆)).

Fig. 3. (a) Rapport critique h_c/d, et (b) vitesse de sédimentation u_c, des configurations rigides pour $\lambda = 0, 5$ ($N = 4$(□) ou $N = 5$(■)), $\lambda = 1$ ($N = 4$(○) ou $N = 5$(●)) et $\lambda = 2$ ($N = 4$(◇) ou $N = 5$(◆)).

given spacing d. For example, the critical N-particle cluster with ratio d/a_3 settles faster when involving prolate spheroids than when consisting of N spheres.

5. Concluding remarks

The present method nicely recovers previous results for spheres and permits us to deal with non-spherical particles. The exhibited critical steady configurations of $N = 4, 5$ spheres and spheroids are likely to be unstable and the challenging stability analysis of such clusters, assuming a fluid flow of small but non-zero Reynolds number as achieved in [11] for identical spheres lying in the same horizontal plane, is under current investigation.

References

[1] M. Stimson, G.B. Jeffery, The motion of two spheres in a viscous fluid, Proc. Roy. Soc. London A 111 (1926) 110–116.
[2] A.J. Goldman, R.G. Cox, H. Brenner, The slow motion of two identical arbitrarily oriented spheres through a viscous fluid, Chem. Engrg. Sci. 21 (1966) 1151–1170.
[3] E. Wacholder, N.F. Sather, The hydrodynamic interaction of two unequal spheres moving under gravity through a quiescent fluid, J. Fluid Mech. 65 (1974) 417–437.
[4] Q. Hassonjee, P. Ganatos, R. Pfeffer, A strong-interaction theory for the motion of arbitrary three-dimensional clusters of spherical particles at low Reynolds number, J. Fluid Mech. 197 (1988) 1–37.
[5] M.J. Gluckman, R. Pfeffer, R. Weinbaum, A new technique for treating multiparticle slow viscous flow: axisymmetric flow past spheres and spheroids, J. Fluid Mech. 50 (1971) 705–740.
[6] W.H. Liao, D.A. Krueger, Multipole expansion calculation of slow viscous flow about spheroids of different sizes, J. Fluid Mech. 96 (1980) 223–241.
[7] S. Kim, S.J. Karrila, Microhydrodynamics: Principles and Selected Applications, Butterworth, 1991.
[8] J. Happel, H. Brenner, Low Reynolds Number Hydrodynamics, Martinus Nijhoff, 1973.
[9] C. Pozrikidis, Boundary Integral and Singularity Methods for Linearized Viscous Flow, Cambridge University Press, 1992.
[10] M. Bonnet, Boundary Integral Equation Methods for Solids and Fluids, John Wiley & Sons, 1999.
[11] F.P. Bretherton, Inertial effects on clusters of spheres falling in a viscous fluid, J. Fluid Mech. 20 (1964) 401–410.